



Published in final edited form as:

*Biochemistry*. 2021 September 07; 60(35): 2672–2676. doi:10.1021/acs.biochem.1c00535.

## Adenylate Kinase-Catalyzed Reaction of AMP in Pieces: Enzyme Activation for Phosphoryl Transfer to Phosphite Dianion

**Patrick L. Fernandez,**

Department of Chemistry, University at Buffalo, The State University of New York at Buffalo, Buffalo, New York 14260-3000, United States

**John P. Richard**

Department of Chemistry, University at Buffalo, The State University of New York at Buffalo, Buffalo, New York 14260-3000, United States

### Abstract

The binding of adenosine 5'-triphosphate (ATP) and adenosine 5'-monophosphate (AMP) to adenylate kinase (AdK) drives closure of lids over the substrate adenosyl groups. We test the hypothesis that this conformational change activates AdK for catalysis. The rate constants for *Homo sapiens* adenylate kinase 1 (*HsAdK1*)-catalyzed phosphoryl group transfer to AMP,  $k_{\text{cat}}/K_{\text{m}} = 7.0 \times 10^6 \text{ M}^{-1} \text{ s}^{-1}$ , and phosphite dianion,  $(k_{\text{HPi}})_{\text{obs}} = 1 \times 10^{-4} \text{ M}^{-1} \text{ s}^{-1}$ , show that the binding energy of the adenosyl group effects a  $7.0 \times 10^{10}$ -fold rate acceleration of phosphoryl transfer from ATP. The third-order rate constant of  $k_{\text{cat}}/K_{\text{HPi}}K_{\text{EA}} = 260 \text{ M}^{-2} \text{ s}^{-1}$  for 1-( $\beta$ -D-erythrofuransyl)adenine (EA)-activated phosphoryl transfer to phosphite dianion was determined, and the isohypophosphate reaction product characterized by  $^{31}\text{P}$  NMR. The results demonstrate: (i) a 14.7 kcal/mol stabilization of the transition state for phosphoryl transfer by the adenosyl group of AMP and a  $2.6 \times 10^6$ -fold rate acceleration from the EA-driven conformational change, and (ii) the recovery of 8.7 kcal/mol of this transition state stabilization for EA-activated phosphoryl transfer from ATP to phosphite.

### Graphical Abstract

**Corresponding Author:** John P. Richard – Department of Chemistry, University at Buffalo, The State University of New York at Buffalo, Buffalo, New York 14260-3000, United States; jrichard@buffalo.edu.

Author Contributions

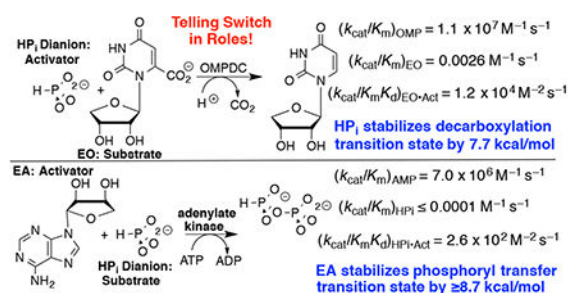
All authors have given approval to the final version of the manuscript.

Supporting Information

The Supporting Information is available free of charge on the ACS Publications website.

Experimental Section with (i) the sources of the enzymes and chemicals used in this work, (ii) procedures for the preparation and purification of TEV protease and *HsAdK1*, and (iii) protocol for the determination of kinetic parameters for *HsAdK1*-catalyzed reactions of the whole substrate AMP and the substrate pieces phosphite and EA. Results Section with (i) SDS-PAGE gel for purified TEV protease and *HsAdK1* (Figure S1), (ii) kinetic data for *HsAdK1*-catalyzed reactions of ATP with AMP (Figure S2), and (iii) kinetic data for *HsAdK1*-catalyzed hydrolysis of the ATP (Figure S3A) and for the effect of increasing  $[\text{HPi}]$  on the velocity *HsAdK1*-catalyzed conversion of ATP to ADP (Figure S3B). (PDF)

The authors declare no competing financial interests.



## Keywords

AK1; P00568; p1 protease; Q0GDU8

The phosphodianion of phosphate monoester substrates for metabolic reactions provides *ca.* 12 kcal/mol of binding energy for stabilization of transition states for enzyme-catalyzed proton transfer, hydride transfer,<sup>1, 2</sup> decarboxylation,<sup>2, 3</sup> and phosphoryl transfer reactions.<sup>4</sup> From 33–66% of this binding energy is utilized in phosphite dianion activation of these enzymes for catalysis of the reactions of phosphodianion truncated substrates.<sup>1–5</sup> Our model to rationalize the reactions of substrate pieces can be generalized to any enzyme that undergoes a substrate-driven conformational change,<sup>6</sup> but phosphite dianion is the only identified activating substrate piece.

Adenylate kinase (AdK) catalyzes the transfer of a phosphoryl group from ATP to AMP to form two molecules of ADP (Scheme 1). The binding of nucleotide substrates to AdK drives the closure of ATP- and AMP-lids over the substrate adenosine groups.<sup>7</sup> We predict that these protein-adenosine interactions activate AdK for catalysis of phosphoryl transfer, and that AdK is an effective catalyst of the reaction of the AMP pieces 1-( $\beta$ -D-erythrofuranosyl)adenine (EA) and phosphite dianion. This is a reversal of the roles of phosphite dianion (substrate) and truncated nucleoside EA (activator) from that for phosphite dianion activation of orotidine monophosphate decarboxylase (OMPDC, Scheme 2).<sup>8</sup>

The commercial sources for all materials, and the methods for the preparation of *Homo sapiens* adenylate kinase 1 (*HsAdK1*) and tobacco etch virus (TEV) protease are given in the Supporting Information (SI). The following protocols are described in the SI: (i) assays for AdK-catalyzed phosphoryl transfer from ATP to AMP, for AdK-catalyzed hydrolysis of ATP, and for unactivated and EA-activated AdK-catalyzed phosphoryl transfer from ATP to phosphite dianion and (ii) protocol for product determination using <sup>31</sup>P NMR.

His<sub>6</sub>-tag labelled *HsAdK1* was expressed in *E. coli*, purified over a Ni<sup>2+</sup>-column, and the His<sub>6</sub>-tag removed by tobacco etch virus (TEV)-protease. The purified *HsAdK1* showed a single band by SDS-PAGE (Figure S1). The initial velocity,  $v_0$ , at 25 °C for *HsAdK1*-catalyzed phosphoryl transfer from ATP to AMP was determined by a standard enzyme assay (SI).<sup>9</sup> Figure S2 shows a plot of  $v_0/[E]$  against AMP for *HsAdK1*-catalyzed phosphoryl transfer from 1 mM ATP (saturating)<sup>10</sup> to AMP to form 2 ADPs at 25 °C

and pH 7.5, which gave the kinetic parameters  $k_{\text{cat}}/K_{\text{m}} = (7.0 \pm 0.4) \times 10^6 \text{ M}^{-1} \text{ s}^{-1}$ ,  $k_{\text{cat}} = 475 \pm 8 \text{ s}^{-1}$  and  $K_{\text{m}} = 68 \pm 4 \text{ }\mu\text{M}$ .

*HsAdK1*-catalyzed hydrolysis of ATP to ADP was monitored by coupling the formation of ADP to the oxidation of NADH by pyruvate, catalyzed by lactate dehydrogenase. Figure S3A shows the dependence of  $v_0$  on  $[\text{HsAdK1}]$  for catalysis of hydrolysis of 1 mM ATP (saturating)<sup>10</sup> to form ADP. The slope of this correlation,  $k_{\text{hyd}} = 5 \times 10^{-6} \text{ s}^{-1}$ , is similar to  $k_{\text{hyd}} = 2 \times 10^{-6} \text{ s}^{-1}$  reported for adenylate kinase from *E. coli*.<sup>7</sup>

Figure S3B shows the increase in  $k_{\text{hyd}} = 5 \times 10^{-6} \text{ s}^{-1}$  for *HsAdK1*-catalyzed (72  $\mu\text{M}$ ) conversion of ATP (1 mM) to ADP in the presence of increasing concentrations of phosphite dianion. The slope of this correlation,  $(k_{\text{HPPi}})_{\text{obs}} = (9.9 \pm 0.3) \times 10^{-5} \text{ M}^{-1} \text{ s}^{-1}$ , is the sum of the rate constants for *HsAdK1*-catalyzed phosphoryl transfer from ATP to phosphite to form isohypophosphate ( $\text{HPPi}$ ),  $(k_{\text{HPPi}})_{\text{E}}$ , and for activation of the *HsAdK1*-catalyzed hydrolysis reaction by a specific salt effect,  $(k_{\text{HPPi}})_{\text{salt}}$ . The formation of ADP by the reaction of phosphite with ATP (Scheme 3) would result in a low yield of  $\text{HPPi}$ , undetectable by the <sup>31</sup>P analytical methods described below. Therefore, the value of  $(k_{\text{HPPi}})_{\text{obs}} = (9.9 \pm 0.3) \times 10^{-5} \text{ M}^{-1} \text{ s}^{-1}$  (Figure S3B) sets an upper limit of  $(k_{\text{HPPi}})_{\text{E}} = 1 \times 10^{-4} \text{ M}^{-1} \text{ s}^{-1}$  for unactivated *HsAdK1*-catalyzed phosphoryl transfer from ATP to phosphite (Table 1).

The *HsAdK1*-catalyzed conversion of ATP to ADP in the presence of phosphite dianion is strongly activated by EA. Figure 1A shows the effect of increasing  $[\text{EA}]$  on  $(v_{\text{obs}} - v_0)$  for *HsAdK1*-catalyzed (2  $\mu\text{M}$ ) reactions of saturating ATP (1 mM), where  $v_{\text{obs}}$  is the total reaction velocity, and  $v_0$  is a 1.1% correction for the velocity at  $[\text{EA}] = 0 \text{ M}$ . The increase in  $(v_{\text{obs}} - v_0)$  is consistent with EA-activation of *HsAdK1* for catalysis of phosphoryl transfer from ATP to  $\text{HPO}_3^{2-}$  to form  $\text{HPPi}$  (Scheme 3). We confirm this by determining the reaction products using <sup>31</sup>P NMR.

The *HsAdK1*-catalyzed conversion of ATP to ADP in the presence of phosphite dianion was monitored in a 1.0 mL solution in D<sub>2</sub>O that contains 50 mM TEA (pD 7.5), 10 mM EA, 3 mM MgCl<sub>2</sub>, 30 mM KCl, 25 mM phosphite (93% dianion),<sup>1</sup> 1 mM ATP, 30 mM phosphoenolpyruvate (PEP), 10 mM phosphonoacetate (<sup>31</sup>P-standard), 1 U pyruvate kinase, and 67  $\mu\text{M}$  *HsAdK1*. This reaction was monitored continuously for 16 h at 25 °C by <sup>31</sup>P NMR spectroscopy on a Varian Inova 500 MHz spectrometer, as described in the SI. Figure 2 shows the relevant changes in the <sup>31</sup>P NMR spectra during this time. The integrated areas for the singlet for PEP (−0.62 ppm) and doublet for phosphite (3.05 ppm, d,  $^1J_{\text{PH}} = 568 \text{ Hz}$ ) decrease, as peaks for  $\text{HPPi}$  appear (−4.50 ppm, dd,  $^1J_{\text{PH}} = 646 \text{ Hz}$ ,  $^2J_{\text{PP}} = 17 \text{ Hz}$ ; −5.44 ppm, d,  $^2J_{\text{PP}} = 17 \text{ Hz}$ ).<sup>11</sup> No inorganic phosphate from adenylate-kinase catalyzed hydrolysis of ATP, or from hydrolysis of  $\text{HPPi}$  was detected. This is consistent with the published 12 h half-time for hydrolysis of  $\text{HPPi}$  at 60 °C and pH 7.4.<sup>11</sup>

The sum of the normalized <sup>31</sup>P peaks areas for the reactants PEP and phosphite ( $A_{\text{R}}$ ) and the  $\text{HPPi}$  product ( $A_{\text{P}}$ ) were determined using a constant peak area ( $A_{\text{S}}$ ) for the phosphonoacetate standard. There is no significant change in the sum of normalized areas of peaks for reactants and products during the reaction. Figure 3 compares the time courses for the decrease in the fraction of PEP and phosphite reactants remaining ( $A_{\text{i}} = A_{\text{R}}$ ) with

the increase in the fraction of reactants converted to HPP<sub>i</sub> ( $A_i = A_p$ ), with normalization of ( $A_R + A_p$ ). The solid lines in Figure 3 show the fit of these data to the rate equation for the apparent first-order conversion of (30 mM PEP + 25 mM phosphite) to HPP<sub>i</sub>, using a rate constant of  $k_{\text{obs}} = 0.16 \text{ h}^{-1}$  and reaction end-points of 22 mM HPP<sub>i</sub> and 11 mM (PEP + phosphite). These fits show that the reactants are converted to HPP<sub>i</sub> as essentially the exclusive product.

Figure 3 shows that *HsAdK*1-catalyzed phosphoryl transfer from ATP to phosphite dianion to form HPP<sub>i</sub> can account for essentially the entire increase in ( $v_{\text{obs}} - v_o$ ) from Figure 1A. The solid lines for Figures 1A show the nonlinear least squares fits of the kinetic data to eq 1, derived for Scheme 4, assuming  $K_{\text{HPi}} \gg [\text{HP}_i]$  and using the values of  $(k_{\text{cat}}/K_{\text{EA}})_{\text{obs}}$  determined for reactions at different  $[\text{HPO}_3^{2-}]$ . Figure 1B shows the linear plot (eq 2) of values of  $(k_{\text{cat}}/K_{\text{EA}})_{\text{obs}}$  from Figure 1A, against  $[\text{HPO}_3^{2-}]$ . The slope of this correlation is  $(k_{\text{cat}})_{\text{HPi}\cdot\text{EA}}/K_{\text{HPi}}K_{\text{EA}} = (2.58 \pm 0.05) \times 10^2 \text{ M}^{-2} \text{ s}^{-1}$  (Table 1).

Table 1 summarizes data that defines the role of the adenosyl group of AMP in activating *HsAdK*1 for catalysis of phosphoryl transfer from enzyme saturated with ATP (1 mM). The values of  $k_{\text{cat}}/K_m = 7.0 \times 10^6 \text{ M}^{-1} \text{ s}^{-1}$  and  $(k_{\text{HPi}})_E = 1 \times 10^{-4} \text{ M}^{-1} \text{ s}^{-1}$ , respectively for the catalyzed reactions of AMP and phosphite dianion show that the AMP adenosyl group is responsible for a  $7.0 \times 10^{10}$ -fold rate acceleration for phosphoryl group transfer. This is a lower limit, because the full AMP binding interactions are probably not expressed at the transition state for the enzyme conformational change, which limits the rate of reaction of AMP.<sup>7</sup> This corresponds to a 14.7 kcal/mol stabilization of the transition state for phosphoryl transfer by the AMP adenosyl group. The ratio of the rate constants for *HsAdK*1-catalyzed phosphoryl transfer from ATP to  $\text{HPO}_3^{2-}$  in the presence and absence of the EA activator,  $2.6 \times 10^6 \text{ M}$ , shows that 8.7 kcal/mol of the adenosyl binding energy is recovered as stabilization of the transition state by the activator. This binding energy is utilized to hold AdK in an active closed conformation.<sup>6, 12–15</sup> By comparison, the transition state for OMPDC-catalyzed decarboxylation is stabilized 12 kcal/mol by interactions with the OMP phosphodianion and 19 kcal/mol by interactions with the OMP ribosyl and orotate moieties.<sup>8</sup>

Inorganic triphosphate binds weakly to chicken muscle adenylate kinase ( $K_d = 1 \text{ mM}$ ) and undergoes phosphoryl transfer to AMP with  $k_{\text{cat}}$  that is *ca* ( $10^4$ – $10^5$ )-fold smaller than for the reaction of ATP.<sup>16</sup> This shows that the adenosyl group of ATP is essential for optimal phosphoryl donor activity. *HsAdK*1 shows a higher specificity for the phosphoryl acceptor AMP compared to the donor ATP,<sup>17</sup> which suggests a larger activating adenosyl binding energy for the acceptor compared with the donor nucleotide.

$$\frac{v_{\text{obs}} - v_o}{[E]} = \frac{(k_{\text{cat}})_{\text{HPi}\cdot\text{EA}}[\text{EA}][\text{HPO}_3^{2-}]}{K_{\text{HPi}}K_{\text{EA}} + K_{\text{HPi}}[\text{EA}]} \quad (1)$$

$$(k_{\text{cat}}/K_{\text{EA}})_{\text{obs}} = \frac{(k_{\text{cat}})_{\text{HPi}\cdot\text{EA}}[\text{HPO}_3^{2-}]}{K_{\text{HPi}}K_{\text{EA}}} \quad (2)$$

Adenylate kinase functions in muscle tissues to maintain an equilibrium concentration of ATP, ADP, and AMP in order to optimize [ATP] under conditions of energy stress, created by the rapid myosin-catalyzed hydrolysis of ATP. This important function creates pressure to optimize enzyme activity, similar to that for the glycolytic enzyme TIM.<sup>19, 20</sup> In these and other cases, the pressure to optimize catalytic activity has driven evolution of protein motifs, where substrate binding energy is utilized to drive large, enzyme-activating, conformation changes.<sup>2, 6</sup>

X-ray crystal structures for AdK show that the adenosyl group of AMP sits distant from the reacting phosphates, and is held at the enzyme by hydrogen bonds with protein side chains and backbone amides.<sup>21, 22</sup> The ligand phosphates interact with many cationic amino acid side chains and backbone amides, so that the activator-driven conformational changes move disordered polar groups into positions that provide for optimal stabilizing electrostatic interactions with the phosphate oxygens at the transition state for *HsAdK1*-catalyzed phosphoryl transfer.<sup>23</sup> We propose that the 8.7 kcal/mol transition state stabilization from binding of the EA activator is due to the incremental tightening of many stabilizing polar interactions that result from the ligand-driven enzyme conformational change.

## Supplementary Material

Refer to Web version on PubMed Central for supplementary material.

## Funding Sources

The authors acknowledge the National Institutes of Health Grant GM134881 for support of this work.

## ABBREVIATIONS

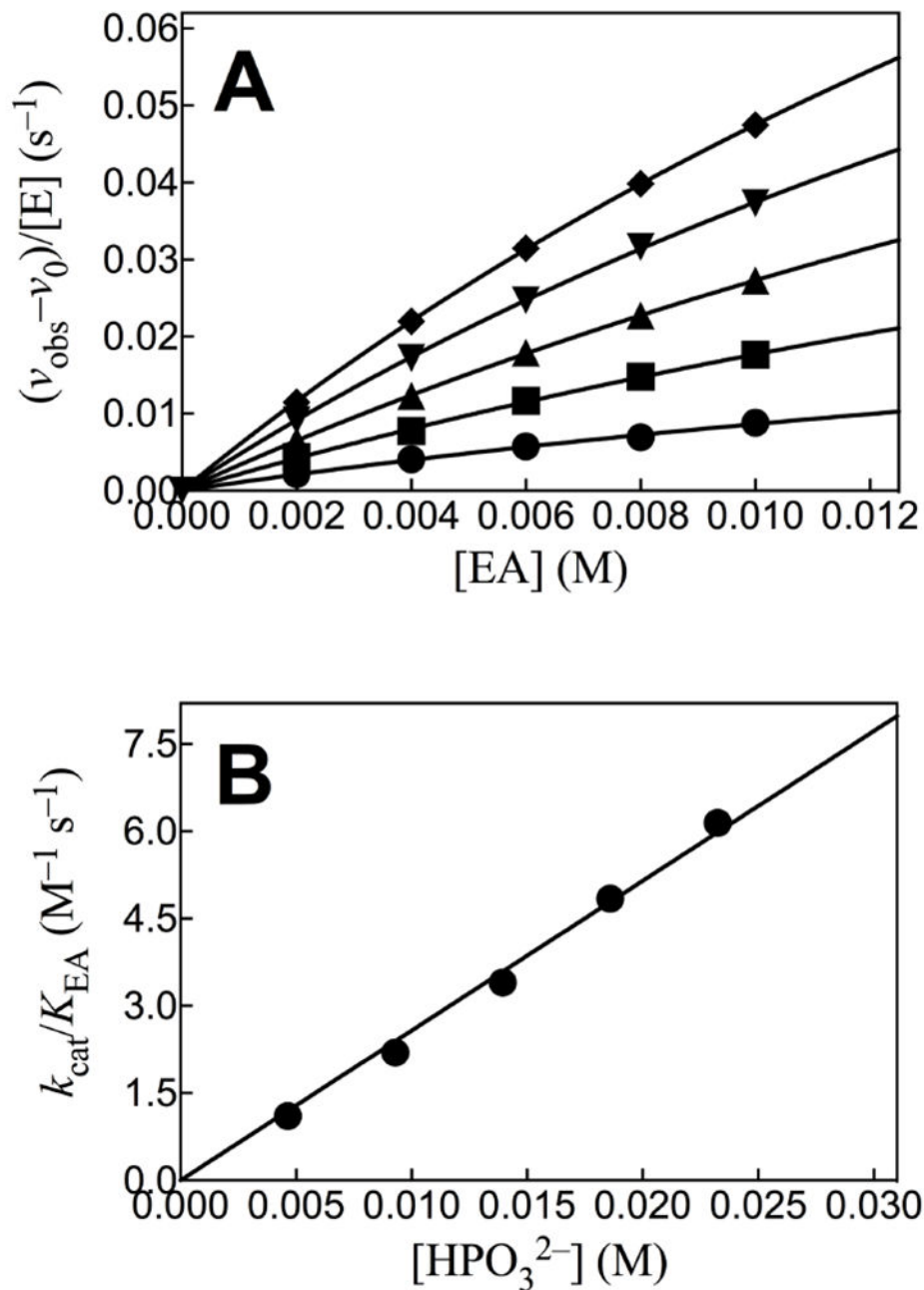
<b>AdK</b>	adenylate kinase
<b>AMP</b>	adenosine 5'-monophosphate
<b>ADP</b>	adenosine 5'-diphosphate
<b>ATP</b>	adenosine 5'-triphosphate
<b><i>HsAdK1</i></b>	<i>Homo sapiens</i> adenylate kinase 1
<b>EA</b>	1-(β-D-erythrofuranosyl)adenine
<b>HPP<sub>i</sub></b>	isohypophosphate
<b>OMP</b>	orotidine 5'-monophosphate
<b>OMPDC</b>	orotidine 5'-monophosphate decarboxylase
<b>SI</b>	Supporting Information
<b>TEA</b>	triethanolamine
<b>TEV</b>	tobacco etch virus

**TIM** triosephosphate isomerase**REFERENCES**

- [1]. Tsang W-Y, Amyes TL, and Richard JP (2008) A Substrate in Pieces: Allosteric Activation of Glycerol 3-Phosphate Dehydrogenase (NAD<sup>+</sup>) by Phosphite Dianion. *Biochemistry* 47, 4575–4582. [PubMed: 18376850]
- [2]. Fernandez PL, Nagorski RW, Cristobal JR, Amyes TL, and Richard JP (2021) Phosphodianion Activation of Enzymes for Catalysis of Central Metabolic Reactions. *J. Am. Chem. Soc* 143, 2694–2698 [PubMed: 33560827]
- [3]. Amyes TL, Richard JP, and Tait JJ (2005) Activation of orotidine 5'-monophosphate decarboxylase by phosphite dianion: The whole substrate is the sum of two parts. *J. Am. Chem. Soc* 127, 15708–15709. [PubMed: 16277505]
- [4]. Ray WJ Jr., Long JW, and Owens JD (1976) An analysis of the substrate-induced rate effect in the phosphoglucomutase system. *Biochemistry* 15, 4006–4017. [PubMed: 963019]
- [5]. Amyes TL, and Richard JP (2007) Enzymatic catalysis of proton transfer at carbon: activation of triosephosphate isomerase by phosphite dianion. *Biochemistry* 46, 5841–5854. [PubMed: 17444661]
- [6]. Richard JP (2019) Protein Flexibility and Stiffness Enable Efficient Enzymatic Catalysis. *J. Am. Chem. Soc* 141, 3320–3331. [PubMed: 30703322]
- [7]. Kerns SJ, Agafonov RV, Cho Y-J, Pontiggia F, Otten R, Pachov DV, Kutter S, Phung LA, Murphy PN, Thai V, Alber T, Hagan MF, and Kern D (2015) The energy landscape of adenylate kinase during catalysis. *Nature* 22, 124–131.
- [8]. Richard JP, Amyes TL, and Reyes AC (2018) Orotidine 5'-Monophosphate Decarboxylase: Probing the Limits of the Possible for Enzyme Catalysis. *Acc. Chem. Res* 51, 960–969. [PubMed: 29595949]
- [9]. Rhoads DG, and Lowenstein JM (1968) Initial Velocity and Equilibrium Kinetics of Myokinase. *J. Biol. Chem* 243, 3963–3972. [PubMed: 5690818]
- [10]. Sheng XR, Li X, and Pan XM (1999) An Iso-random Bi Bi Mechanism for Adenylate Kinase. *J. Biol. Chem* 274, 22238–22242. [PubMed: 10428790]
- [11]. Carroll RL, and Mesmer RE (1967) Isohypophosphate: Kinetics of Hydrolysis and Potentiometric and Nuclear Magnetic Resonance Studies on the Acidity and Complexing. *Inorg. Chem* 6, 1137–1142.
- [12]. Amyes TL, Malabanan MM, Zhai X, Reyes AC, and Richard JP (2017) Enzyme activation through the utilization of intrinsic dianion binding energy. *Prot. Eng. Des. & Sel* 30, 157–165.
- [13]. Thomas JA, and Koshland DE Jr. (1960) Competitive inhibition by substrate during enzyme action. Evidence for the induced-fit theory. *J. Am. Chem. Soc* 82, 3329–3333.
- [14]. Koshland DE Jr. (1958) Application of a Theory of Enzyme Specificity to Protein Synthesis. *Proc. Natl. Acad. Sci. U. S. A* 44, 98–104. [PubMed: 16590179]
- [15]. Amyes TL, and Richard JP (2013) Specificity in transition state binding: The Pauling model revisited. *Biochemistry* 52, 2021–2035. [PubMed: 23327224]
- [16]. Sanders CR, Tian G, and Tsai MD (1989) Mechanism of adenylate kinase. Is there a relationship between local substrate dynamics, and local binding energy, and the catalytic mechanism? *Biochemistry* 28, 9028–9043. [PubMed: 2557915]
- [17]. Panayiotou C, Solaroli N, and Karlsson A (2014) The many isoforms of human adenylate kinases. *Int. J. Biochem. & Cell. Biol* 49, 75–83. [PubMed: 24495878]
- [18]. Reyes AC, Zhai X, Morgan KT, Reinhardt CJ, Amyes TL, and Richard JP (2015) The Activating Oxydianion Binding Domain for Enzyme-Catalyzed Proton Transfer, Hydride Transfer and Decarboxylation: Specificity and Enzyme Architecture. *J. Am. Chem. Soc* 137, 1372–1382. [PubMed: 25555107]
- [19]. Knowles JR, and Albery WJ (1977) Perfection in enzyme catalysis: the energetics of triosephosphate isomerase. *Acc. Chem. Res* 10, 105–111.

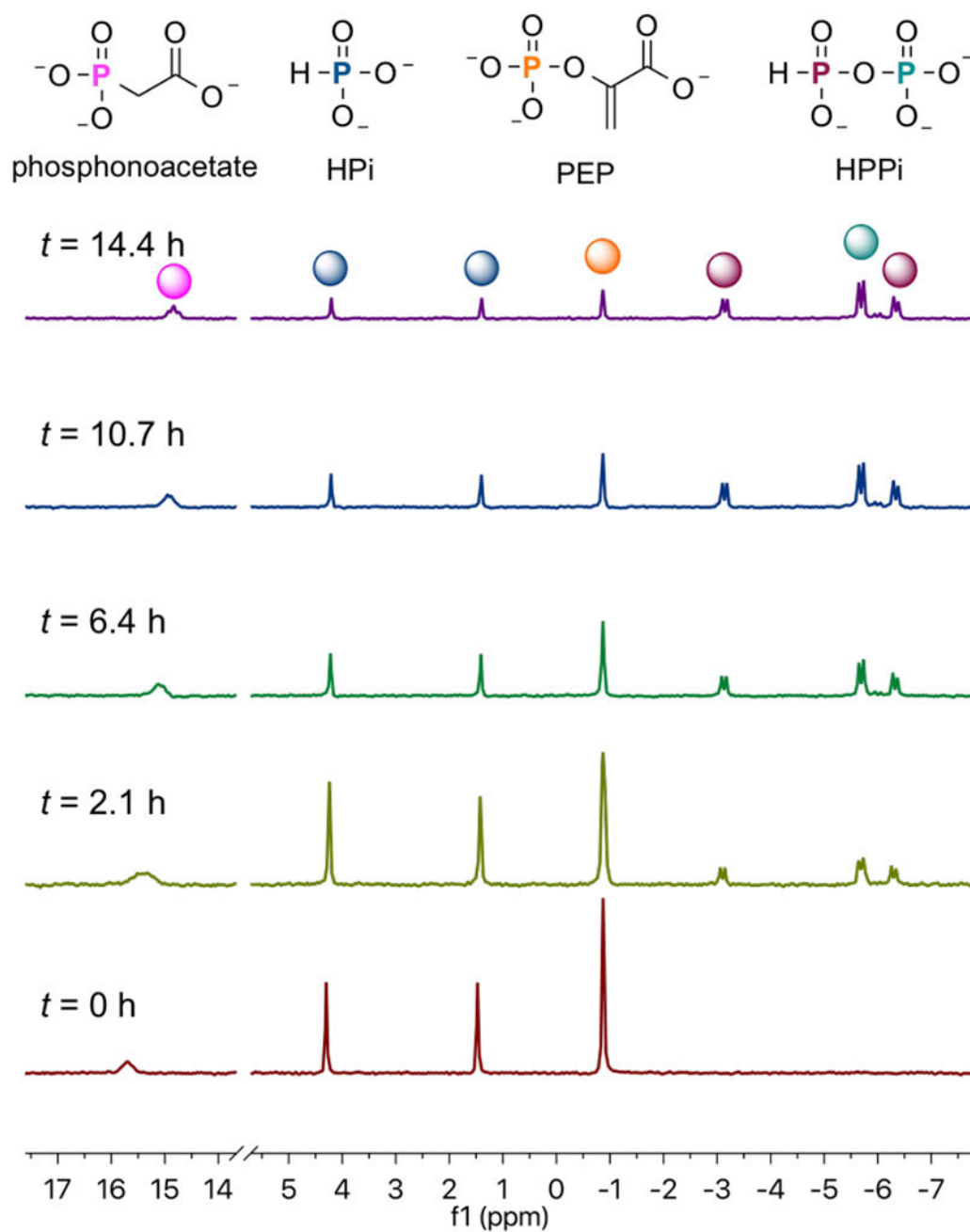
- [20]. Albery WJ, and Knowles JR (1976) Evolution of enzyme function and the development of catalytic efficiency. *Biochemistry* 15, 5631–5640. [PubMed: 999839]
- [21]. Bellinzoni M, Haouz A, Graña M, Munier-Lehmann H, Shepard W, and Alzari PM (2006) The crystal structure of *Mycobacterium tuberculosis* adenylate kinase in complex with two molecules of ADP and  $Mg^{2+}$  supports an associative mechanism for phosphoryl transfer. *Prot. Sci* 15, 1489–1493.
- [22]. Müller CW, and Schulz GE (1992) Structure of the complex between adenylate kinase from *Escherichia coli* and the inhibitor Ap5A refined at 1.9 Å resolution: A model for a catalytic transition state. *J. Mol. Biol* 224, 159–177. [PubMed: 1548697]
- [23]. Warshel A, Sharma PK, Kato M, Xiang Y, Liu H, and Olsson MHM (2006) Electrostatic basis for enzyme catalysis. *Chem. Rev* 106, 3210–3235. [PubMed: 16895325]



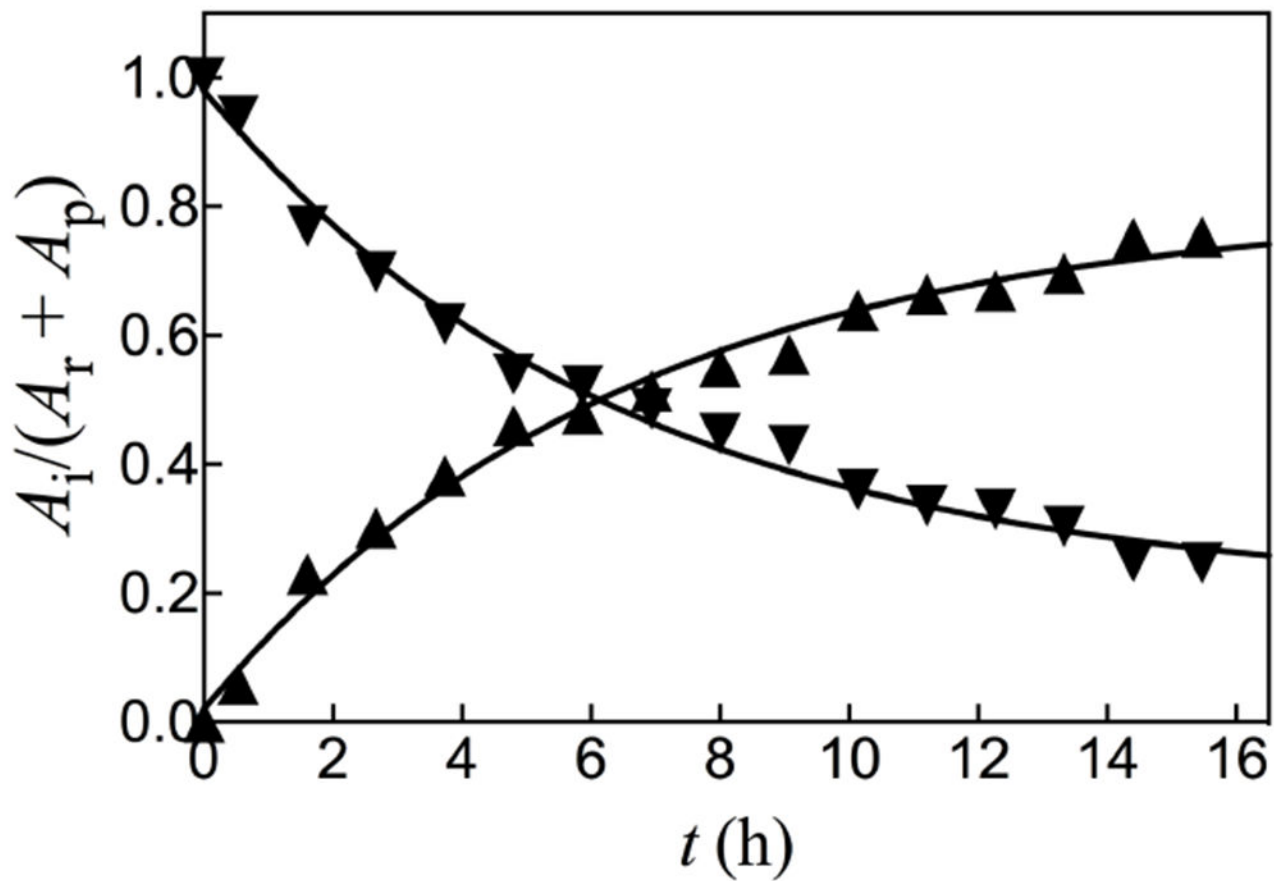
**Figure 1.**

(A) The effect of increasing [EA] on the velocity for *HsAdK1*-catalyzed reactions of ATP (1 mM) at 25 °C. Key: ♦, 25 mM [HP<sub>i</sub>]<sub>T</sub>, (93% dianion); ▼, 20 mM [HP<sub>i</sub>]<sub>T</sub>; ▲, 15 mM [HP<sub>i</sub>]<sub>T</sub>; ■, 10 mM [HP<sub>i</sub>]<sub>T</sub>; ●, 5 mM [HP<sub>i</sub>]<sub>T</sub>. (B) The effect of increasing [HPO<sub>3</sub><sup>2-</sup>] on the values of  $(k_{\text{cat}}/K_{\text{EA}})_{\text{obs}}$  determined for Figure 1A.

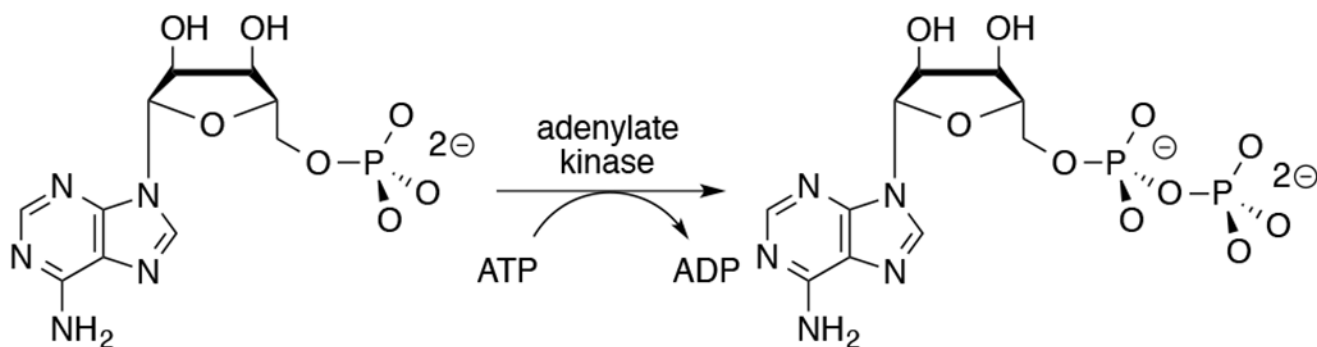




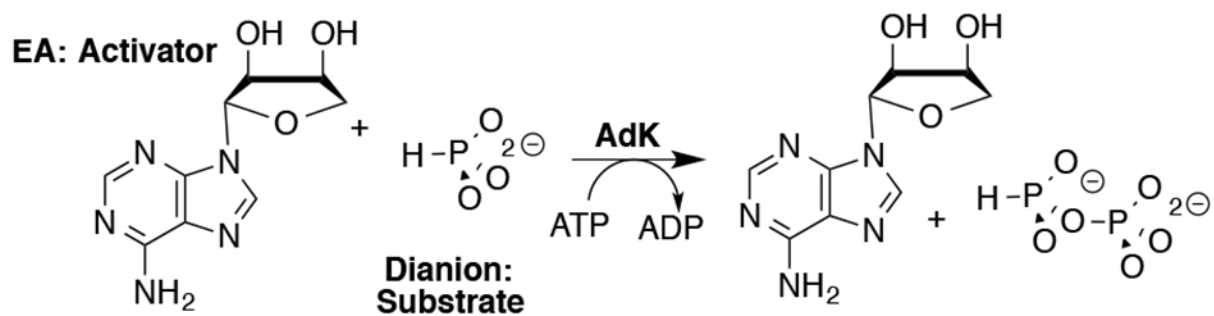
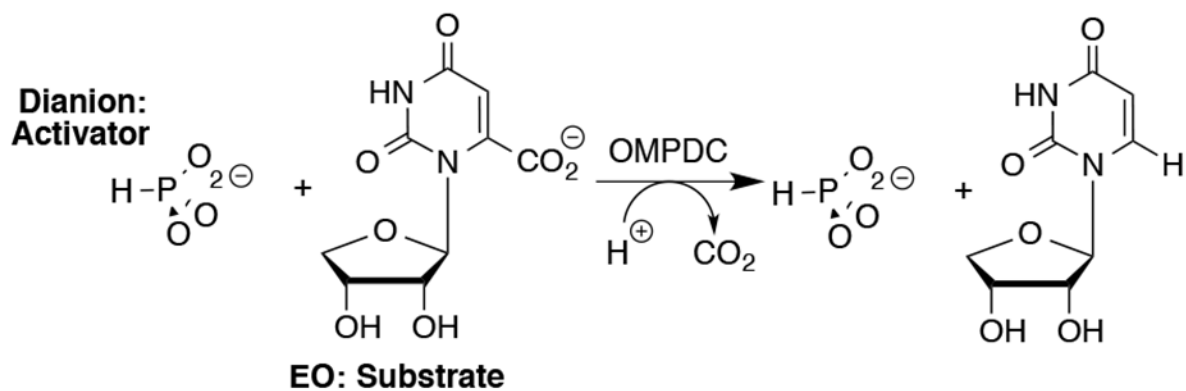
**Figure 2.**  $^{31}\text{P}$  NMR spectra that show the change with time in the areas of the peaks  $A_R$  at  $-0.62$  and  $3.05$  ppm for PEP and phosphite reactants, and  $A_P$  at  $-4.50$  and  $5.44$  ppm for  $\text{HPPi}$  product of EA-activated *HsAdK1*-catalyzed reactions (Scheme 3).



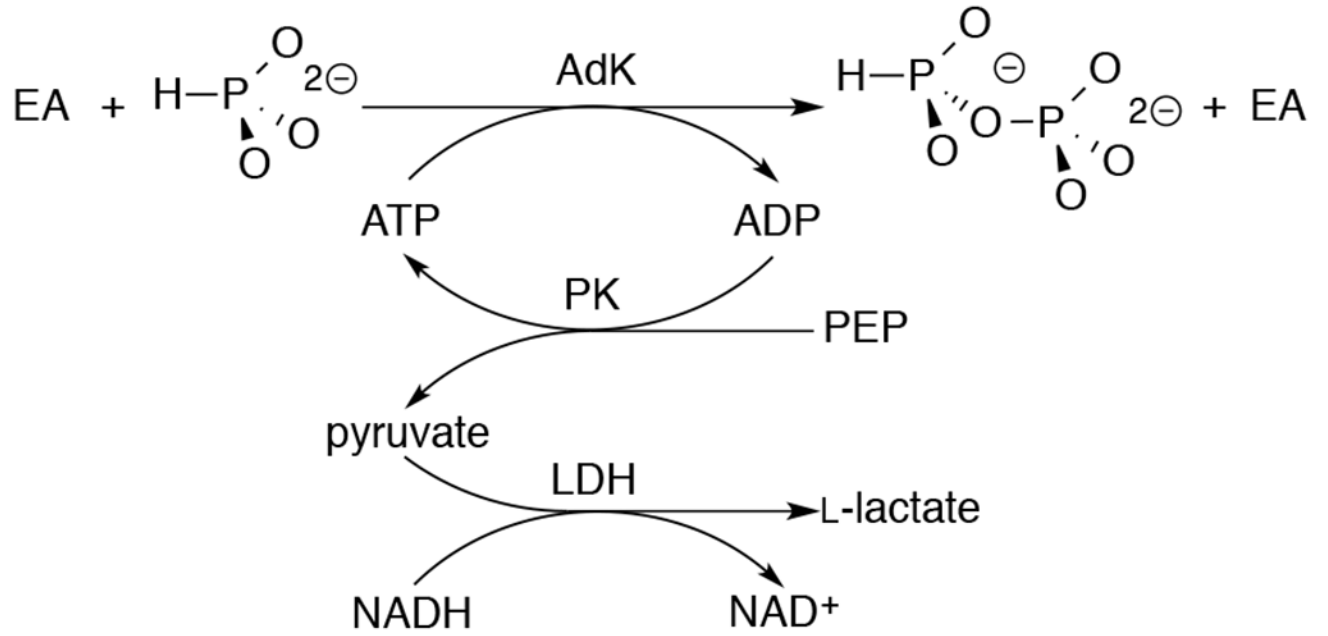
**Figure 3.**  
The fractions of reactants PEP and phosphite remaining (▼,  $A_i = A_R$ ) and product HPP<sub>i</sub> formed (▲,  $A_i = A_P$ ) at time  $t$ , determined by integration of the peaks from Figure 2.



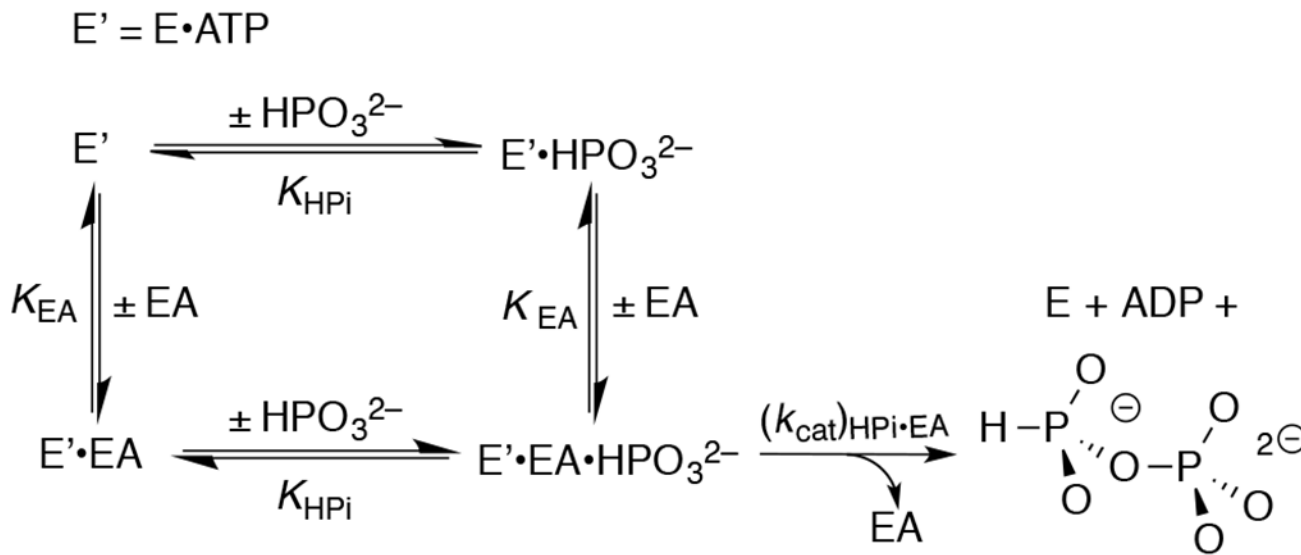
**Scheme 1.**  
Adenylate Kinase-Catalyzed Phosphoryl Transfer from ATP to ADP.

**Scheme 2.**

Roles of Dianion and Nucleoside (EO and EA) Substrate Pieces in Reactions Catalyzed by OMPDC and AdK.

**Scheme 3.**

Assay to Monitor AdK-Catalyzed Phosphoryl Transfer from ATP to Phosphite Dianion.



**Scheme 4.**  
Kinetic Mechanism for Activation of *HsAdK1*-Catalyzed Phosphoryl Transfer from ATP to Phosphite Dianion by the Substrate Piece EA.

**Table 1.**

Rate Constants and Transition-State Binding Energies  $G^\ddagger$  for *HsAdK1*-Catalyzed Phosphoryl Transfer from 1.0 mM ATP to AMP and to Phosphite Dianion.<sup>a</sup>

Phosphoryl Acceptor	Kinetic Parameter	$G^\ddagger$ (kcal/mol) <sup>b</sup>
AMP	$k_{\text{cat}}/K_m$ $(7.0 \pm 0.4) \times 10^6 \text{ M}^{-1} \text{ s}^{-1}$	14.7 <sup>c</sup>
$\text{HPO}_3^{2-} + \text{EA}$	$(k_{\text{cat}})_{\text{HPi+EA}}/K_{\text{HPi}}K_{\text{EA}}$ $(2.58 \pm 0.05) \times 10^2 \text{ M}^{-2} \text{ s}^{-1}$ <sup>d</sup>	8.7 <sup>e</sup>
$\text{HPO}_3^{2-}$	$(k_{\text{HPi}})_E$ $1.0 \times 10^{-4} \text{ M}^{-1} \text{ s}^{-1}$ <sup>f</sup>	

<sup>a</sup>At 25 °C and pH 7.5.

<sup>b</sup>Calculated from the ratio of rate constants for *HsAdK1*-catalyzed reactions of AMP and the substrate piece ( $\text{HPO}_3^{2-}$ ) or pieces ( $\text{HPO}_3^{2-} + \text{EA}$ ).

<sup>c</sup>Assuming similar intrinsic nucleophilic reactivities for AMP and phosphite dianion.

<sup>d</sup>Determined from the fit of data from Figure 1B to eq 2.

<sup>e</sup>Calculated from the ratio of rate constant for *HsAdK1*-catalyzed reactions of phosphite in the presence and absence of EA.<sup>18</sup>

<sup>f</sup>The slope from Figure S3B (see text).